

Developing velocity sensitivity in a model neuron by local synaptic plasticity

Minija Tamosiunaite · Bernd Porr ·
Florentin Wörgötter

Received: 30 June 2006 / Accepted: 12 February 2007 / Published online: 13 April 2007
© Springer-Verlag 2007

Abstract Sensor neurons, like those in the visual cortex, display specific functional properties, e.g., tuning for the orientation, direction and velocity of a moving stimulus. It is still unclear how these properties arise from the processing of the inputs which converge at a given cell. Specifically, little is known how such properties can develop by ways of synaptic plasticity. In this study we investigate the hypothesis that velocity sensitivity can develop at a neuron from different types of synaptic plasticity at different dendritic substructures. Specifically we are implementing spike-timing

dependent plasticity at one dendritic branch and conventional long-term potentiation at another branch, both driven by dendritic spikes triggered by moving inputs. In the first part of the study, we show how velocity sensitivity can arise from such a spatially localized difference in the plasticity. In the second part we show how this scenario is augmented by the interaction between dendritic spikes and back-propagating spikes also at different dendritic branches. Recent theoretical (Saudargiene et al. in *Neural Comput* 16:595–626, 2004) and experimental (Froemke et al. in *Nature* 434:221–225, 2005) results on spatially localized plasticity suggest that such processes may play a major role in determining how synapses will change depending on their site. The current study suggests that such mechanisms could be used to develop the functional specificities of a neuron.

M. Tamosiunaite
Department of Psychology, University of Stirling,
Stirling FK9 4LA, Scotland

M. Tamosiunaite
Department of Informatics, Vytautas Magnus University,
Kaunas, Lithuania
e-mail: m.tamosiunaite@if.vdu.lt

B. Porr
Department of Electronics and Electrical Engineering,
University of Glasgow, Glasgow GT12 8LT, Scotland

F. Wörgötter
Bernstein Center for Computational Neuroscience,
University of Göttingen, Göttingen, Germany

F. Wörgötter
Department of Psychology, University of Stirling,
Stirling FK9 4LA, Scotland
e-mail: worgott@bccn-goettingen.de

B. Porr (✉)
Department of Electronics and Electrical Engineering,
University of Glasgow, Room 519, Rankine Building,
Oakfield Avenue, Glasgow G12 8LT, Scotland
e-mail: b.porr@elec.gla.ac.uk
URL: <http://www.berndporr.me.uk/>
URL: <http://www.linux-usb-daq.co.uk/>

1 Introduction

There is growing evidence that synaptic plasticity can be different for different synapses at the same neuron. Thus, depending on the location at the dendrite or soma different forms of plasticity can co-exist at a cell and plasticity appears to be most often a spatially local process (Froemke et al. 2005). This is partly due to the fact that dendritic compartments are often to a large degree decoupled from each other such that local, site-specific interactions can take place in independence making each single dendrite functionally similar to a whole computational network (Mel 1994; Poirazi et al. 2003). Furthermore it is known that the electrical and chemical signals which drive synaptic change can be very different at different sites (Häusser and Mel 2003; Golding et al. 2002).

Two types of long-lasting synaptic changes are in general observed, long term potentiation (LTP) and long term

depression (LTD) (Bliss and Lomo 1970, 1973; Bliss and Gardner-Edwin 1973). Which type of plasticity actually occurs at a given synapse, however, depends on the synapse type, the order in which pre- and post-synaptic signals arrive, the type of transmitter involved and often also on other modulatory substances.

To induce plasticity a strong depolarization is necessary at most synapses presumably for the unblocking of NMDA-channels (Debanne et al. 1998; Chen et al. 1999; Nishiyama et al. 2000; Sjöström et al. 2001; Kovalchuk et al. 2000; Bi 2002). Such a depolarization can be achieved by back-propagating (BP) somatic action potentials. However, at most cells these signals are only strong close to the soma and become longer in duration and smaller in amplitude while propagating into the dendritic tree (Magee and Johnston 1997; Linden 1999). This attenuation (Stuart and Spruston 1998; Häusser and Mel 2003) will lead to the fact that in distal dendritic parts, BP spikes may not anymore be strong enough to drive plasticity and instead synaptic changes may be triggered by local dendritic Na^+ - and Ca^{2+} channel dependent spikes (Golding et al. 2002; Larkum et al. 2001). Many times it can be assumed here that dendritic spikes (D-spikes) are initiated by localized but strong cooperative synaptic inputs.

The effects discussed above indicate that the different shapes of BP- and dendritic-spikes, which change along the dendrite, should lead to different post-synaptic influences on plasticity depending on the dendritic site.

This hypothesis had been theoretically investigated in a few of our older studies. By ways of modeling synaptic plasticity with a differential Hebbian learning rule, we were able to show that different weight change curves will be obtained depending on the shape of the post-synaptic signals. At that time we had speculated that: “Such local, site-specific plasticity may be important because at a single neuron different rules for synaptic plasticity can coexist this way. Networks, which can implement such “local learning properties”, will certainly demonstrate substantially enriched computational properties” (Saudargiene et al. 2005).

It is the goal of this article to provide some theoretical evidence substantiating this speculation and we will use this mechanism to show that it is possible to gradually develop certain functional properties at a neuron. It will be shown that spatially localized synaptic plasticity can lead to a differential effect subdividing the responses from different dendrites in a way which creates a neuron that is sensitive to the velocity of a simulated visual stimulus.

After introducing our formalism, we will in the first part of this paper show some results about local plasticity, demonstrating how different types of synaptic changes can arise in a spatially localized way. This is partly a summary from our older work (Saudargiene et al. 2004, 2005). In the second part we will then first discuss how different D-spikes arising at different parts of a two-branch dendrite will lead to

increasing velocity sensitivity at the simulated neuron. Finally we will also discuss what may happen if at some point during development a global signal, from a BP-spike, will influence both branches at the same time.

2 Methods

We will first introduce our synapse model before we describe the more complex full setup of the modeled circuit.

2.1 Synapse model, plasticity rule and saturation characteristics

Our synapse (Fig. 1) consists of AMPA as well as NMDA influences. The AMPA influence is only used to drive the soma, it does not enter plasticity. The NMDA influence constitutes the pre-synaptic part of our learning rule.

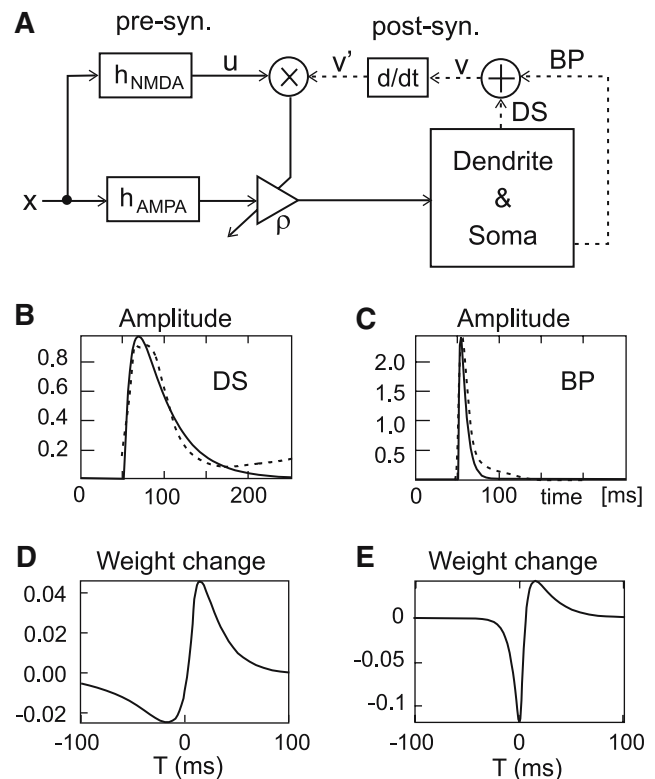


Fig. 1 The synapse model (a) and examples of D- and BP-spikes (b, c), where we have superimposed two real signals recorded in different studies (dashed) as well as (d, e) their model weight change curves. DS stands for D-spike, BP for a BP-spike, ρ is the synaptic weight, x , u and v the different pre- and post-synaptic signals explained in the text. **b** D-spike with $\tau = 235$ ms, dashed is superimposed a D-spike taken from Fig. 3b in Saudargiene et al. (2005). **c** BP-spike with $\tau = 40$ ms, dashed is superimposed a BP-spike taken from Fig. 3a in Saudargiene et al. (2005). **d, e** STDP curves for **b, c**. **d** STDP curve obtained with the model D-spike, **e** STDP curve from the model BP spike

The post-synaptic part arises mainly from dendritic spikes (D-spikes), which, however, can be summed also with the influence from a back-propagating (BP-) spike. Detailed equations for the pre- and post-synaptic signals will be given below. The model assumes that input synapses are clustered, so that a longitudinal dendritic dimension may be neglected, and all the synapses in a cluster share the same membrane voltage (and other membrane properties) at each particular moment in time.

We will mainly analyze a combination of spike-timing dependent plasticity (STDP) and LTP and both types of plasticity are implemented using the same differential Hebbian learning rule (Porr and Wörgötter 2003; Saudargiene et al. 2004):

$$\frac{d\rho}{dt} = \mu u_{\text{NMDA}}(t) \dot{v}(t) \tag{1}$$

where ρ denotes the synaptic weight of synapse ρ , μ the learning rate and $\dot{v}(t)$ is the temporal derivative of the conjoint post-synaptic influences. Learning rate $\mu = 0.03$ was used.

Weights were kept in the interval $[0,1]$ using a hysteresis type saturation function. The saturation was achieved applying a weight-dependent nonlinear transformation for the weight modification term $\Delta\rho$ obtained in one integration step of Eq. 1. If the weights were increasing towards one, or decreasing towards zero, the following function was applied to the weight change $\Delta\rho$ (see inset in Fig. 2):

$$\Delta\rho_{tr} = \frac{1}{1 + \frac{1-\rho}{\rho} \exp(-\Delta\rho)} - \rho \tag{2}$$

The opposite cases, which capture growth of small weights and decrease of big weights, were kept linear. The transition between linear and hysteresis-saturated parts was placed at a weight value of $\rho = 0.5$. In the linear part weight modification $\Delta\rho$ was multiplied by a constant: $\Delta\rho_{tr} = 0.25\Delta\rho$, to keep the derivative at the boundary between linear and nonlinear parts smooth.

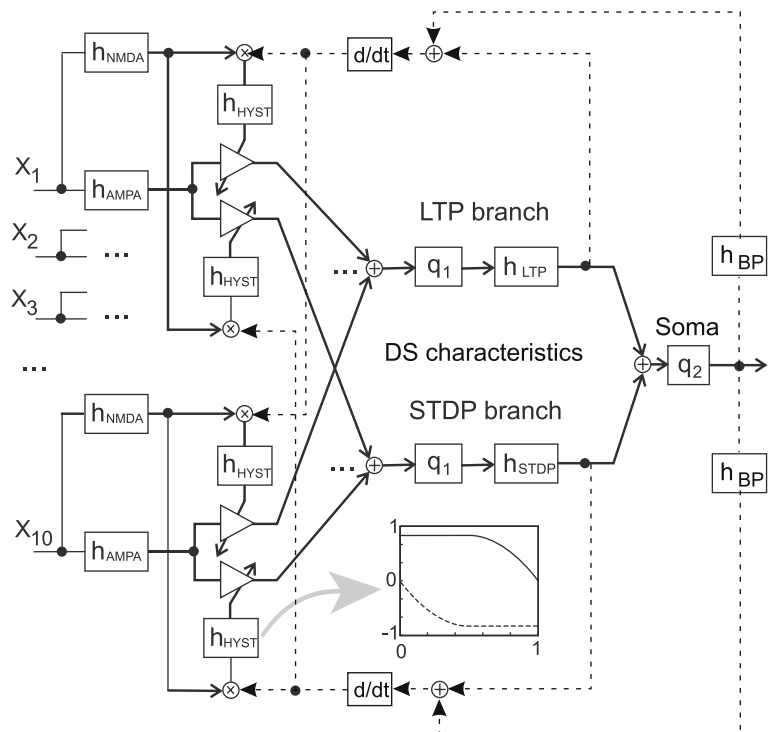
In real systems some weight stabilization mechanism is employed to keep weights from excessive saturation (Bi and Poo 1998) and this is mimicked by our hysteresis function.

Panels (b–e) of Fig. 1 show typical examples of D- and BP-spikes and the weight change curves derived from them. Real D- and BP-spike examples taken from the literature are depicted by the dashed curves, which demonstrates the similarity of the modeled to the real signals. Evidently, D- and BP-spikes lead to differently shaped weight change curves. Specifically, and as shown previously (Saudargiene et al. 2004), an output $v(t)$ with a shallow rising flank will predominantly lead to LTP, while one with a steep rising flank results in STDP.

2.2 Circuit model

We model AMPA and NMDA receptor activation signals, dendritic spikes initiated by inputs to the synaptic clusters, and the back-propagating spikes originating after the cell has fired. Figure 2 shows the complete setup. The model contains two dendritic branches which are receiving the same set of ten inputs x_1, \dots, x_{10} . At each individual branch dendritic

Fig. 2 Block diagram of the model neuron. Each of the ten inputs x_1, \dots, x_{10} targets two synapses, one for the LTP-, the other one for the STDP-branch, leading to a total of 20 weights. Filters h_{AMPA} and h_{NMDA} are used for initiation of a dendritic spike, and to influence learning. Weight change is saturated through a hysteresis-type filter h_{HYST} , which is characterized in the inset. We define q_1 as the threshold for eliciting a dendritic spike. Filter h_{LTP} is used for shaping a shallow and h_{STDP} for a steep dendritic spike. The threshold for cell firing is called q_2 . In the inset the hysteresis of a weight change on the weight itself is specified: solid line—weight change during weight increase, dashed line—during weight decrease (see Sect. 2)



spikes are elicited following the summation of several AMPA signals passing threshold q_1 . We assume the NMDA influence on dendritic spike can be neglected because the contribution of NMDA potentials to the total membrane potential is substantially smaller than that of AMPA channels.

Cell firing is not explicitly modeled but said to be achieved when the summation of several dendritic spikes at the cell soma has passed threshold q_2 . This leads to a BP-spike. Progression of signals along a dendrite is also not modeled explicitly, but expressed by means of delays. All signal shapes, which influence plasticity, are obtained by appropriate filters (see below).

As shape and timing interplay is the most important aspect of this study, we provide realistic timing in milliseconds for the employed signals. Absolute signal amplitudes are irrelevant and only arbitrary units are used here.

2.2.1 Model equations

We define it below:

$$u_{\text{NMDA}}(t) = x(t) \times h_{\text{NMDA}}(t) \tag{3}$$

$$u_{\text{AMPA}}(t) = x(t) \times h_{\text{AMPA}}(t) \tag{4}$$

where $x(t)$ is a spike train given in the usual way as a sequence of δ -functions.

Filter functions $h(t)$ define the signal shapes of D- and BP-spikes. We use Eq. 5 for modelling the shapes of the AMPA and NMDA channel responses, as well as those of back-propagating spikes and some forms of dendritic spikes:

$$h(t) = \frac{e^{-2\pi t/\tau} - e^{-8\pi t/\tau}}{6\pi/\tau} \tag{5}$$

where τ determines the total duration of the pulse. The ratio between rise and fall time is 1:4.

For modeling the AMPA channel potentials (h_{AMPA}) a filter with $\tau = 6$ ms was used, for modeling the NMDA channel potentials (h_{NMDA}) we use $\tau = 120$ ms, for dendritic spikes (h_{DS}) we set $\tau = 235$ ms and for back-propagating spikes (h_{BP}) a filter with $\tau = 40$ ms is employed.

Note, in this study, we have approximated the NMDA characteristic by a non-voltage dependent filter function. In conjunction with STDP, this simplification is justified by the analytical solutions for STDP curves derived in [Saudargiene et al. \(2005\)](#), which show that voltage dependency induces only a second-order effect on the shape of the STDP curve.

To get a pure LTP-case a wider and shallower rising dendritic spike has been employed:

$$h(t) = t^p \left(e^{-bt} - e^{-at} \right) \tag{6}$$

with $p = 2$, a rise time of $a = 1/1$ ms and a decay time of $b = 1/40$ ms following [Saudargiene et al. \(2004\)](#).

To actually elicit a D- or BP-spike, we define two summation processes (1) a local dendritic-summation process and (2) a somatic summation process.

(1) Dendritic summation is given by:

$$y(t) = \sum_j \rho^j u_{\text{AMPA}}^j(t) \tag{7}$$

where we sum over all synaptic inputs j .

We elicit a D-spike if this process exceeds a certain threshold q_1 , hence if at time-points t_i we have $y(t_i) > q_1$ then we elicit a D-spike v_{DS} , receiving a train of signals:

$$v_{\text{DS}}(t) = \sum_i \delta(t - t_i) \times h_{\text{DS}}(t) \tag{8}$$

Outside the convolution, v_{DS} is set to zero.

(2) In a similar way, at the soma a BP-spike $v_{\text{BP}}(t)$ will be elicited if the signals that arrive at the soma exceed threshold q_2 . Hence, if at time-point t_i we find that $\sum_k v_{\text{DS}}^k(t_i) > q_2$, where k is the number of inputs, then we elicit a BP-spike v_{BP} also here receiving a train of signals:

$$v_{\text{BP}}(t) = \sum_i \delta(t - t_i) \times h_{\text{BP}}(t) \tag{9}$$

3 Developing a velocity sensitive neuron using spatially separated learning rules

Let us consider a model neuron with only two dendritic branches, where on one of the branches an LTP- and on the other one an STDP-rule drives the learning (Fig. 3). Both dendritic branches get inputs from the same stimulus

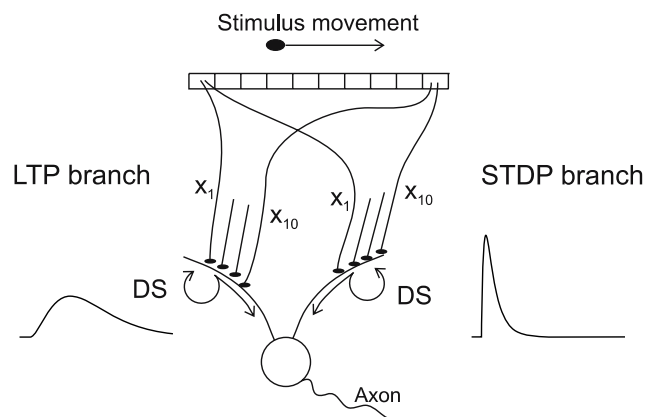


Fig. 3 Model neuron with two dendritic branches. We assume that each branch gets input from an elongated sensor field containing ten sensors (called “pixels”). The pixel signals arrive at the dendrite driving one synapse each on the left and on the right branch top. Dendritic spikes (DS) drive local learning and travel towards the soma to fire the cell. A shallow dendritic spike is used to obtain LTP-type learning on the left branch, and a steep dendritic spike is used on the right branch to get STDP

moving along a one-dimensional sensor field, hence the inputs reach the dendrite strictly ordered in time. While we do not explicitly simulate space in our model, this setup effectively emulates a space to time transformation and leads to summation effects on the dendrite. Note, it would also be possible to replace the LTP branch with an LTD-dominated branch. As will be discussed below (see Sect. 4), the development of velocity sensitivity relies on the differential effects at the STPD branch, where the other branch plays a smaller role.

As described above in this simplified model each dendritic branch gets ten inputs from adjacent pixels of the sensor field. The output signal in the form of a dendritic spike on each branch is generated when the sum of AMPA receptor-like input signals at that branch reaches a specified threshold. Thus inputs on the dendritic branch occur in a specific temporal relation as compared to the output: the first inputs arrive before the output in the form of a dendritic spike has emerged while the last come after it. In the LTP-case all weights are expected to grow, as the whole group of inputs is close enough correlated, while for the STDP setting only the first few weights grow while the other weights shrink.

The model cell fires when a sum of two dendritic spikes goes beyond threshold q_2 (Fig. 2). The threshold is adjusted so that a single dendritic spike is not enough to fire the cell, hence, cooperation of dendritic spikes is required.

Thus, the cell is designed to fire when two conditions are fulfilled: (1) dendritic spikes, both, for the LTP and the STDP branches are present and (2) the time interval between them is relatively small. Both conditions in the current design are easier to achieve for larger velocities, and both mechanisms take part in creating the specificity of the detector.

For training of the model neuron, stimuli moving at varying velocities were applied. For each trial, the interval between excitations was obtained from a *uniform* distribution ranging from 2 to 12 ms/pixel (corresponding to a velocity range from $\frac{1}{2}$ to $\frac{1}{12}$ pixel/ms, although not uniformly distributed in the velocity dimension). Additional noise from an interval of ± 3 ms/pixel (or equivalently $\pm \frac{1}{3}$ pixel/ms) was added to disperse the timings between adjacent pixels or even interchange the spike order in some cases. The noise has been added, both, to reflect possible realistic noise influences and to ease reaching thresholds in early learning stages when weights are still small. This creates a rather high degree of variability. Stimuli moving in both directions defined by negative intervals between adjacent pixel excitations with intervals ranging from -1 to 9 , -3 to 7 or -5 to 5 ms/pixel (corresponding to velocities: -1 to $\frac{1}{9}$, $-\frac{1}{3}$ to $\frac{1}{7}$, and $-\frac{1}{5}$ to $\frac{1}{5}$ pixel/ms) were investigated as well.

Learning was initiated with all weight values 0.5. Threshold q_1 was kept at the level where 2–4 roughly simultaneous inputs were needed to initiate a dendritic spike

at the beginning of learning for the greatest velocities. Hence, for smaller velocities even more simultaneous inputs are needed to initiate a D-spike. Threshold q_2 for cell firing was kept at the level where a single dendritic spike was not enough to initiate the cell firing, as mentioned earlier. A range of thresholds, both, for dendritic spike initiation as well as cell firing, was investigated. A low learning rate of $\mu = 0.03$ was used. This way the model mostly operated in the linear region or with only slight saturation of weight growth during several thousand excitation trials.

Apart from this basic setup, two more types of modified models were analyzed.

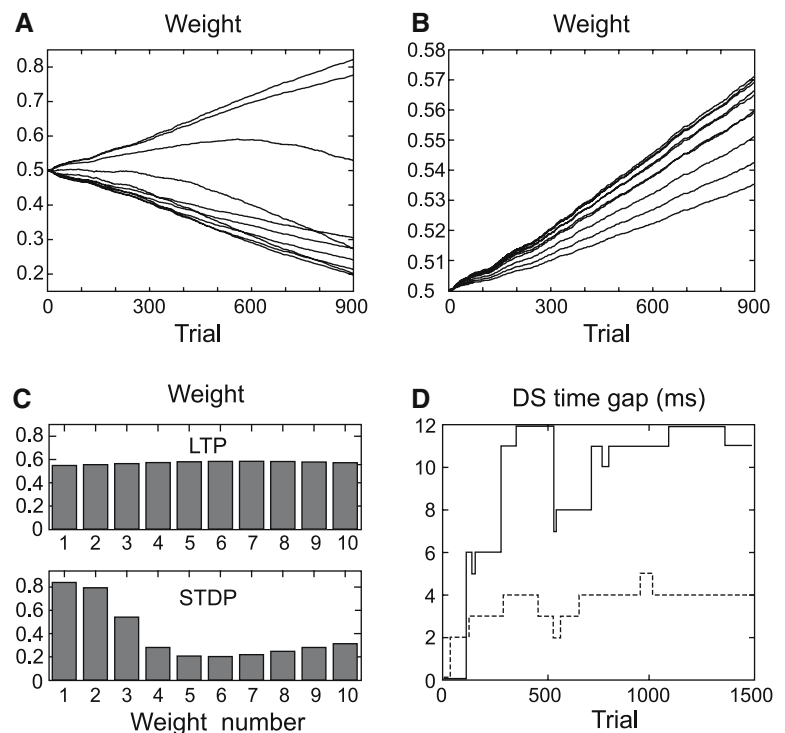
1. In the first modification we investigated the effect of an additional back-propagating (BP) spike on the learning. Here again two cases were analyzed: the BP-spike reaches the STDP cluster, or the BP-spike reaches both clusters. It has been suggested that STDP more likely happens at synapses closer to the soma, whereas pure LTP like plasticity can more easily be observed at distal dendrites (Saudargiene et al. 2004). Hence, either the BP-spike reaches both clusters or rather only the STDP one. The BP-spike was modeled to be shorter than a dendritic spike ($\tau = 40$ ms as compared to 235 ms), but higher in amplitude. To make effects more comparable, BPs spikes were normalized to the same integral area as the used D-spikes.
2. In a second modification, we assumed that both dendritic spikes were identical (STDP type), but on one of the branches the D-spike was supplemented with a BP-spike. This was done to investigate an initially similar situation where only later an asymmetry through the added BP-spike arises.

3.1 Results for the velocity detector development

In the experiment where the detector neuron was trained with no added BP-spikes (basic model), weights growth was approximately linear, as obtained from an experiment with the stimulus 900 times crossing the sensory field (900 trials) with different velocities in the same direction. Learning showed almost no saturation effects due to the small learning rate. The development of the two clusters of weights is presented in Fig. 5a, b. Weights on the LTP branch stopped at very similar values (Fig. 5b, c) at the end of the experiment, with minimally bigger values for the central synapses, while for the STDP branch the biggest weights are obtained (as expected) at the first synapses relative to the movement direction (Fig. 4a, c).

The temporal distance between two dendritic spikes on the two branches increases with learning. This happens as for the STDP setting the first weights increase relatively

Fig. 4 Developing a velocity detector. **a** Development of STDP weights; **b** of LTP weights; **c** final weight distributions, LTP *upper part*, STDP—*lower part*. **d** Development of the time lag between dendritic spikes for the LTP and STDP branches. Solid line for velocity $\frac{1}{6}$ pixel/ms and *dashed line* for a velocity of $\frac{1}{3}$ pixel/ms. Learning was performed with velocities variable in the interval $\frac{1}{12} - \frac{1}{2}$ pixel/ms. D-spike filters followed Eq. 5 with $\tau = 117$ ms for the STDP branch, and Eq. 6 for the LTP branch. AMPA signal filters were derived from Eq. 5 with $\tau = 20$ ms, NMDA: $\tau = 117$ ms, thresholds $q_1 = 0.25$, $q_2 = 3.39$, learning rate $\mu = 0.03$



strongly and the first inputs require less and less “help” from the subsequent inputs to produce a dendritic spike. Thus on the STDP branch a dendritic spike comes increasingly earlier in the course of learning. For the LTP branch the relative weighting does not change during learning, consequently its spike always comes later. This time gap increase is demonstrated for two test velocities in Fig. 4d. For slower velocities the development of the inter-spike time gap is a fraction slower, but the time gap itself reaches greater values (solid vs. dashed line in Fig. 4d). This is the core effect leading to the development of a velocity detection mechanism in the models presented here.

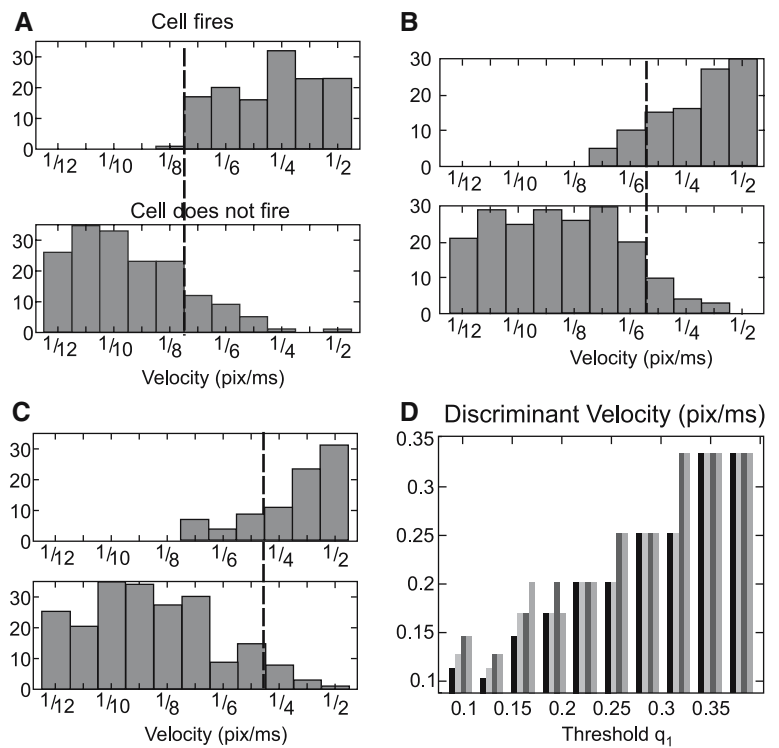
As a consequence, the detector model cell was firing a somatic spike for bigger velocities and was silent for smaller ones. The distribution of cell firing (or not firing) versus stimulus speed, and the development of these distributions in the course of learning is shown in the histograms in Fig. 5a–c. In part Fig. 5a the distribution obtained for the first 300 learning trials, in part Fig. 5b for trials 301–600, and in part Fig. 5c for 601–900 is presented. The so-called *discriminant* boundary between firing and not firing falls between the velocities $\frac{1}{8}$ and $\frac{1}{7}$ pixel/ms in the first 300 trials, between $\frac{1}{6}$ and $\frac{1}{5}$ pixel/ms in the second 300 trials, and between $\frac{1}{5}$ and $\frac{1}{4}$ pixel/ms in the last 300 trials. The shift of the discriminant boundary with learning towards higher velocities shows that the development of a temporal distance between dendritic spikes plays an important role in this design, as the simpler mechanism of firing a cell just by coincident inputs would

not lead to the discriminant shifting towards higher velocities with increasing synaptic strength.

When stimuli were allowed to move in both directions, but one direction was preferred (velocities from -1 to $\frac{1}{9}$, and from $-\frac{1}{3}$ to $\frac{1}{7}$ pixel/ms) the detector properties were developing slower but in the same way as described earlier. Note, also with a symmetrical speed interval from $-\frac{1}{5}$ to $\frac{1}{5}$ pixel/ms detector properties develop but in a slightly different way. On the STDP branch, weights of the first inputs from either side were during half the trials potentiated and during the rest of the trials depressed. Hence, they did not grow on average. Weights in the middle, however, get on average depressed. All weights on the LTP branch, however, grow. As a consequence the D-spike of the LTP branch preceded that on the STDP branch. Due to the shape differences of the LTP and STDP dendritic spikes, this interchanged firing order at some made the cell firing pattern different from the one described above. This leads to the result that this detector is most sensitive for intermediate velocities. The bidirectional case, however, will not be analyzed further.

The detector’s sensitivity for both thresholds q_1 and q_2 was also analyzed (Fig. 5d). Increasing of the threshold q_1 for D-spike formation shifts the discriminant for firing towards higher velocities. The same happens when increasing the threshold q_2 for somatic firing for which the model system is very sensitive: Increase in threshold of around 1% results in substantial discriminant velocity changes of up to 20%.

Fig. 5 Firing characteristics of the velocity detector and its dependency on threshold q_2 . **a** Distribution of velocities when the model cell is firing (upper part) and not firing (lower part) depicting also the discriminants (dashed vertical lines in **a–c**) between these two situations, learning trials 1–300, **b** same as in **a** but learning trials 301–600, **c** same but trials 601–900. Parameters as for Fig. 4. **d** Dependence of the discriminant (obtained from learning trials 101–900) on thresholds q_1 of D-spike formation (x -axis, values from 0.1 to 0.37, step 0.03) and on threshold q_2 for cell firing grouped as quadruplets (q_2 values for each bar quadruplet are 3.37, 3.38, 3.39 and 3.40)



Concerning the effect exerted by q_1 , we observe that two mechanisms interact here: (1) for a higher threshold, the initiation of a dendritic spike is more difficult and possible only for rather synchronous input groups and (2) larger time gaps between dendritic spikes at the LTP and STDP learning clusters develop, which, in turn, reduces the likelihood for coincident D-spikes at the soma.

While the first mechanism is obvious from the explanations above; Table 1 shows what the second effect does. In the table the maximum values of the time gap between the two dendritic spikes developed in a 2,000 trial experiment are given for different thresholds q_1 . For very small thresholds ($q_1 = 0.04$ and smaller, not in table) no separation in time of the two D-spikes develops. With a rising threshold, the inter-D-spike time gap increases. Increase of the time gaps

Table 1 Maximum distance between two D-spikes in ms depending on threshold q_1 . Velocity is given in pixel/ms

q_1	0.10	0.15	0.20	0.25
V				
$\frac{1}{6}$	4	6	12	43
$\frac{1}{5}$	3	5	9	15
$\frac{1}{4}$	2	4	5	8
$\frac{1}{3}$	1	3	3	4
$\frac{1}{2}$	1	2	2	3

between the two D-spikes with higher thresholds q_1 is obtained because of the specific form of the signal used for D-spike initiation which is a sum of low-pass filtered pulses. Their sum's rising phase is steeper and similar on both branches, but shows a more shallow development thereafter, which is different on the two branches. This effect leads, at a high threshold, to considerable time gaps between the D-spikes on both branches.

Varying the shape of the dendritic spike also influences the detector properties. An experiment was performed with varying p in Eq. 6 between 0.05 and 2.05 for only one D-spike, which changes the rising flank of its shape from steep to shallow (Fig. 6a). The other D-spike was kept steep-flanked (Eq. 5 with $\tau = 117$ ms, dashed line in Fig 6a) throughout all experiments. Hence, learning on the shape-manipulated branch was varying from STDP to LTP with increasing p .

With steep flanks speed differentiation was obtained only due to the different likelihood of dendritic spike formation for different stimulus velocities as explained above. For shallow flanks, on the other hand, the cell firing threshold q_2 added its considerable influence. The change of the discriminant firing velocities for the analyzed forms (Fig. 6b) shows a trend towards bigger velocities with a more LTP-like learning characteristic on the shape manipulated branch. For very small values of p the curve also drops which is due to more subtle effect of the fine interplay between the different filter forms in the used model/plasticity setup.

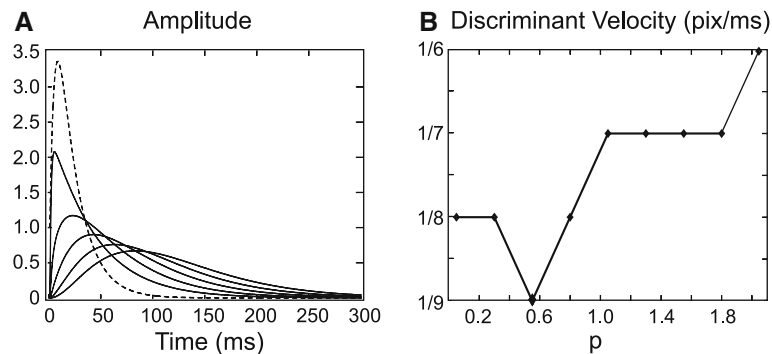


Fig. 6 Influence of the filter shape. **a** Varying filter shapes on one learning branch, *solid lines* with p values 0.05, 0.55, 1.05, 1.55, and 2.05 increasing from left to right, normalized to have constant area under the curve, and the constant filter shape used for the other branch (Eq. 5

with $\tau = 117$ ms, *dashed line*), velocity interval; $\frac{1}{12} - \frac{1}{2}$ pixel/ms. **b** Discriminant between velocities for cell firing and not firing for different shapes, versus filter parameter p , $q_1 = 0.2$, $q_2 = 3.39$, $\mu = 0.03$

In Fig. 7 we finally look at the two modifications of the basic setup obtained following the ideas from the first part of the study about the possible interplay of dendritic and back-propagating spikes:

1. First, we investigate the influence of an additional BP-spike—first influencing only the STDP branch. We find that the time gap between both D-spikes developed faster and increased in absolute value in comparison to the case without BP-spike (see Fig. 7a, b for a comparison). The discriminant obtained with a BP-spike is shifted towards bigger velocities (Fig. 7c, compare to Fig. 5b). This effect can be expected, as adding an even steeper BP-spike on top of D-spike, which is responsible for STDP, will drive the learning curve even more towards an STDP characteristic. This makes learning still more selective for the first weights in the series of inputs and consequently the two weight distributions become more different (not shown). In the case with a BP-spike added to both clusters, the difference between the initiation times of the two dendritic spikes became smaller and the discriminant was shifted towards slower velocities (Fig. 7d).

2. In the case where both branches are driven by steeply rising dendritic spikes and adding a BP-spike only to one of the branches, learning could not be exactly attributed to LTP-STDP differences. Both learning rules were starting with and continuing to have an STDP characteristic, yet different: the one with the BP-spike was even more selective for the first inputs. Due to the different characteristics, different weight distributions were obtained (not shown), which still were able to yield the necessary time gaps (Fig. 7e) required to develop a velocity detector (Fig. 7f).

4 Discussion

In this study we have shown that it is possible to develop certain functional properties (velocity tuning) in a single

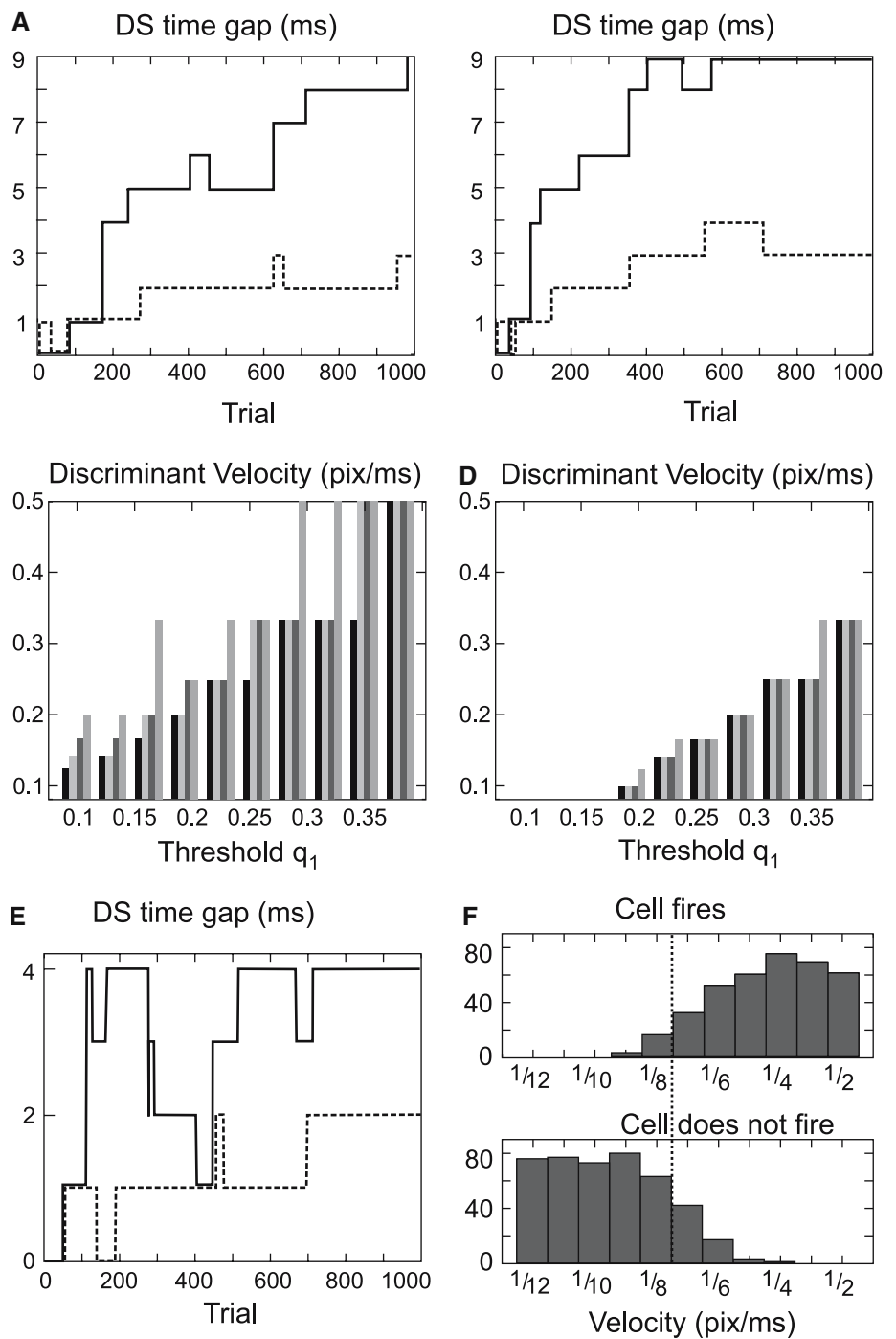
neuron from developing interactions between its dendrites. We would like to first discuss some limitations of our model and in the final paragraphs embed our study in the existing literature on velocity- and directional-tuning.

4.1 Limitations of our model

The model used here relies on a state-variable description of STDP or LTP and does not attempt to model the underlying second messenger chains which are quite complex. A detailed discussion of the limitations that arise from modelling single synapses with such an approach is provided in Saudargiene et al. (2004, 2005), and we will focus here on other aspects which are more directly related to the chosen model level of a small functional dendritic network.

The velocity detector mechanism proposed in our study relies on different distributions of weights in different clusters of synapses obtained if those employ different learning rules. As discussed above, velocity sensitivity will arise immediately from different spatial summation properties, where, for example tighter input coincidence (at bigger velocities) might trigger an output, whereas more dispersed inputs will not. This will in our model always create some kind of velocity high-pass tuned cell, which fires only above a certain velocity (Fig. 8). In cortical cells there are, however, also other tuning curves observed, for example a large group follows a velocity low-pass characteristic and many are tuned with a bell shaped curve (Movshon 1975; Orban et al. 1981; Baker 1998). To obtain these characteristics, one needs to also include mechanisms of temporal summation not present in the current model. Temporal summation will be especially effective at low velocities, creating by itself a low-pass tuned cell. Different combinations of such low-pass with high-pass characteristics, obtainable from our model would lead to the required variety of tuning curves.

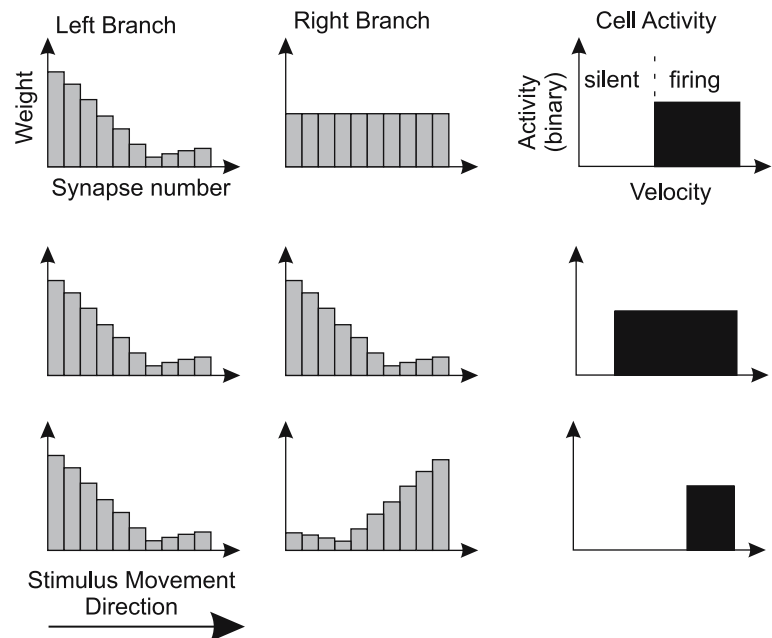
Fig. 7 Influence of BP-spikes. Comparison of time gap development between dendritic spikes on both branches: **a** without BP-spikes and **b** with a BP-spike on the STDP branch only (solid line: $\frac{1}{5}$ pixel/ms; dashed line: $\frac{1}{3}$ pixel/ms). Dependence of the discriminant on thresholds q_1 (x-axis, values from 0.1 to 0.37, step 0.3) and q_2 (quadruplets, from left to right: $q_2 = 3.37, 3.38, 3.39, 3.40$). **c** Here the BP-spike was on the STDP branch and in **d** on both branches. Time gap development and discriminants for a detector with two steep dendritic spikes. Hence, both branches have initially an STDP characteristic with a BP-spike complementing learning on one of the branches. **e** Development of the time gap (solid: $\frac{1}{5}$ pixel/ms, dashed: $\frac{1}{3}$ pixel/ms). **f** Distribution of velocities when the cell fires (upper histogram) and does not fire (lower histogram), which determines the discriminant (dashed line). Simulation parameters: D-spike filters Eq. 5 with $\tau = 117$ ms for the STDP branch, and Eq. 6 with $p = 2$ for the LTP branch (a–d), BP-spike filters Eq. 5 with $\tau = 40$ ms, AMPA signal filters Eq. 5 with $\tau = 20$ ms, NMDA— $\tau = 117$ ms; thresholds $q_1 = 0.25$, $q_2 = 3.39$, learning rate $\mu = 0.03$, velocity range $\frac{1}{12} - \frac{1}{2}$ pixel/ms



One advantageous property of the velocity detector proposed here is that it does not require a specific learning phase, and that it can operate already during learning, as the detection boundary is gradually changing. Furthermore, the detector adapts to different input patterns arriving (whether inputs move from left to right, or reverse, or both sides). Clearly the mechanism, however, is symmetrical and we did not aim to deal with direction selectivity. Furthermore, the model does not contain any weight stabilization mechanisms.

Weight stabilization and a larger dynamic range of the model could be achieved, for example, by including LTD at both branches, which represents a physiologically more realistic situation (Tomita et al. 2005). At the STDP branch, this is already implicitly present through the bimodal characteristic of the STDP window, which would only have to be augmented. The other branch would need to be modified though. On both branches, one would have to make sure that the employed/augmented mechanisms will lead to the

Fig. 8 Influence of the final weight distributions on the firing properties of the model neuron



desired weight stabilization (Royer and Pare 2003). Also there are physiological studies which show that weight growth is intrinsically limited (Bi and Poo 1998). Implementation of such mechanisms, however, have been deliberately excluded to keep this article better focused.

This, however, raises another issue. How would additional plasticity mechanisms change the finally received detector properties? Since we are here dealing only with spatial summation this issues can be analysed by considering three limit cases shown in Fig. 8. Hence, the question can be reduced to asking how (e.g.) additional LTD would lead to different final weight distributions. The situation on top represents the one observed in Fig. 4, where the LTP branch essentially arrives at a flat distribution. The activity of our cell is determined by $y(t) = \sum_j \rho^j u_{\text{AMPA}}^j(t)$, which will lead to a D-spike as soon as y exceeds a threshold. Hence, if the *first-passed-by* synapses (see “Stimulus movement direction”) on both branches are strong enough their combined influence will be enough to push the cell above threshold. This is different in the bottom example, where the first synapses on the right branch are weak and a higher velocity is required to drive the cell. The middle example represents the case which is sensitive to the lowest velocities here. As mentioned above, all these are velocity high-pass cells, which can be altered into low-pass or maximums-tuned cells by adding temporal summation mechanisms to the model.

Of more central interest in the context of this paper was the question how different detector properties can be obtained when a dendritic spike on one branch is supplemented by a back-propagating spike, addressing the interaction of different depolarization sources on a dendrite. In view of the

recent literature on spatially and temporally localized synaptic plasticity it appears to be a timely question to ask how such interactions could influence the functional properties at a neuron, like its velocity tuning.

4.2 Physiology and models of velocity and direction selectivity

The property that visual cortical neurons are selective to specific aspects of the stimulus, like its orientation, its direction of motion and its velocity, has been known since around 1960 (Hubel and Wiesel 1962) and in the next 20 years many papers were published trying to quantify these response specificities (for a review of the older work see Orban 1984).

In our study we were concerned with the development of a velocity sensitive neuronal response from differently developing dendritic branches and in this discussion section we would like to embed our study in the tradition of existing works on velocity sensitivity.

Indeed velocity sensitivity has almost never been considered on its own (Movshon 1975; Orban et al. 1981) but rather normally mostly in conjunction with direction selectivity. The first studies to show direction selective responses were those of Hubel and Wiesel (1962) followed by several other early papers (Barlow and Levick 1965; Pettigrew et al. 1968; Sillito 1977; Hammond 1978). The first models suggested that direction selectivity could be generated from the linear interaction between excitatory and inhibitory influences possibly arising from receptive field subfields, that converge onto a given cell (Emerson and Gerstein 1977; Goodwin et al. 1975; Movshon et al. 1978). Soon, however, it became clear

that a purely linear model does not describe the degree of response depression in the non-preferred direction accurately (Tolhurst and Dean 1991; Reid et al. 1991). Not one of the first, but certainly one of the most appealing models that tries to account for these observations had been presented in a series of studies by David Heeger (1992a,b, 1993) who used the principle of squaring rectified responses to introduce the required non-linearities. His models are especially convincing because of their simple construction and high explanatory value with ideas that are influential to date and taken up even in the most recent models (Kouh and Poggio 2004). Despite the, by modern scientific development processes, almost ancient topic, there are several very recent papers which suggest different additional mechanisms to explain direction and/or velocity sensitivity (Sherman and Spitzer 1995; Hillenbrand and van Hemmen 2001; Priebe and Ferster 2005) supported also by new experimental observations about the structure of visual subfields (Livingstone 1998; Livingstone and Conway 2003; Pack et al. 2006). Direction response asymmetries, however, do not seem to be reflected by possible asymmetries in the anatomical structuring of the corresponding dendrites (Anderson et al. 1999).

In addition to “adult” models for direction and velocity sensitivity there are also some that try to explain how these features could emerge during development (Feidler et al. 1997; Wimbauer et al. 1997a,b). The finding that neuronal plasticity can be temporally asymmetrical (STDP, (Markram et al. 1997; Magee and Johnston 1997)) has led to some boosting of specifically these modelling efforts. After all, it appears straight-forward to use an asymmetrical plasticity mechanism to generate asymmetrical responses. Spike timing dependent plasticity has the nice property that growth or shrinkage of a synapse can be controlled by the temporal order of input and output of a cell which—as soon as they are derived from a moving stimulus—will have different timing dependent on the direction and velocity of the stimulus. Several developmental models for direction and/or velocity sensitivity rely in one way or another on this property (Blais et al. 2000; Buchs and Senn 2002; Senn and Buchs 2003; Shon et al. 2004; Wenisch et al. 2005). These models develop direction and/or velocity sensitivity in a “holistic” way where local dendritic processes do not play a dominant role. This is to some degree intriguing. As discussed above, there exist results that direction and velocity sensitivity arises from the interaction of receptive field subfields which could be of dendritic origin. Also, there is evidence that, in spite of the lack of anatomical specificity (Anderson et al. 1999), there is probably a clear *functional* structure on each dendrite, which leads to local dendritic computations (Mel 1994). In our special case it is, therefore, conceivable that such local dendritic calculations could be the underlying process for the generation of subfields that lead to direction and/or velocity sensitivity. A recent paper by Mo et al. (2004) indeed relates these cor-

tical specifics to the local development of a combination of excitation and shunting inhibition on a dendrite.

In our study we have tried to combine some of the ideas of Shon et al. (2004) about employing STDP for the generation of motion sensitivity with those of Mo et al. (2004) for using local dendritic development and we tried to generate velocity tuning by local dendritic STDP processes.

Acknowledgments The authors acknowledge the support from the European Commission (DRIVSCO) to F.W. and from IBRO to M.T. We are grateful to B. Graham, L. Smith and D. Sterratt for their helpful comments on this manuscript. The authors wish to especially express their thanks to A. Saudargiene for her help at many stages in this project.

References

- Anderson JC, Binzegger T, Kahana O, Martin KA, Segev I (1999) Dendritic asymmetry cannot account for directional responses of neurons in visual cortex. *Nat Neurosci* 2(9):820–824
- Baker CL (1998) Spatial and temporal determinants of directionally selective velocity preference in cat striate cortex neurons. *J Neurophysiol* 59(5):1557–1574
- Barlow HB, Levick WR (1965) The mechanism of directionally selective units in rabbit’s retina. *J Physiol* 178(3):477–504
- Bi GQ (2002) Spatiotemporal specificity of synaptic plasticity: cellular rules and mechanisms. *Biol Cybern* 87:319–332
- Bi GQ, Poo MM (1998) Synaptic modifications in cultured hippocampal neurons: dependence on spike timing, synaptic strength, and postsynaptic cell type. *J Neurosci* 18:10464–10472
- Blais B, Cooper LN, Shouval H (2000) Formation of direction selectivity in natural scene environments. *Neural Comput* 12(5):1057–1066
- Bliss TV, Gardner-Edwin AR (1973) Long-lasting potentiation of synaptic transmission in the dentate area of the unanaesthetized rabbit following stimulation of the perforant path. *J Physiol (Lond)* 232:357–374
- Bliss TV, Lomo T (1970) Plasticity in a monosynaptic cortical pathway. *J Physiol (Lond)* 207:61P
- Bliss TV, Lomo T (1973) Long-lasting potentiation of synaptic transmission in the dentate area of the anaesthetized rabbit following stimulation of the perforant path. *J Physiol (Lond)* 232:331–356
- Buchs NJ, Senn W (2002) Spike-based synaptic plasticity and the emergence of direction selective simple cells: simulation results. *J Comput Neurosci* 13:167–186
- Chen H, Otmakhov N, Strack S, Colbran R, Lisman J (1999) Requirements for LTP induction by pairing in hippocampal CA1 pyramidal cell. *J Neurophysiol* 82:526–532
- Debanne D, Gähwiler B, Thompson S (1998) Long-term synaptic plasticity between pairs of individual CA3 pyramidal cells in rat hippocampal slice cultures. *J Physiol (Lond)* 507:237–247
- Emerson RC, Gerstein GL (1977) Simple striate neurons in the cat. II. Mechanisms underlying directional asymmetry and directional selectivity. *J Neurophysiol* 40(1):136–155
- Feidler JC, Saul AB, A M, Humphrey AL (1997) Hebbian learning and the development of direction selectivity: the role of geniculate response timings. *Network* 8:195–214
- Froemke RC, Poo Mm, Dan Y (2005) Spike-timing-dependent synaptic plasticity depends on dendritic location. *Nature* 434:221–225
- Golding NL, Staff PN, Spurston N (2002) Dendritic spikes as a mechanism for cooperative long-term potentiation. *Nature* 418:326–331
- Goodwin AW, Henry GH, Bishop PO (1975) Direction selectivity of simple striate cells: properties and mechanism. *J Neurophysiol* 38(6):1500–1523

- Hammond P (1978) Directional tuning of complex cells in area 17 of the feline visual cortex. *J Physiol* 285:479–491
- Häusser M, Mel B (2003) Dendrites: bug or feature? *Curr Opin Neurobiol* 13:372–383
- Heeger DJ (1992a) Half-squaring in responses of cat striate cells. *Vis Neurosci* 9(5):427–443
- Heeger DJ (1992b) Normalization of cell responses in cat striate cortex. *Vis Neurosci* 9(2):181–197
- Heeger DJ (1993) Modeling simple-cell direction selectivity with normalized, half-squared, linear operators. *J Neurophysiol* 70(5):1885–1898
- Hillenbrand U, van Hemmen JL (2001) Does corticothalamic feedback control cortical velocity tuning? *Neural Comput* 13(2):327–355
- Hubel DH, Wiesel TN (1962) Receptive fields, binocular interaction and functional architecture in the cat's visual cortex. *J Physiol* 160:106–154
- Kouh M, Poggio T (2004) A general mechanisms for tuning: Gain control circuits underlie tuning of cortical orientation. AIM-2004-031 (MIT Technical Report) <ftp://www.publications.ai.mit.edu/ai-publications/2004/AIM-2004-031.ps>:1–4
- Kovalchuk Y, Eilers J, Lisman J, Konnerth A (2000) NMDA receptor-mediated subthreshold Ca^{2+} -signals in spines of hippocampal neurons. *J Neurosci* 20:1791–1799
- Larkum ME, Zhu JJ, Sakmann B (2001) Dendritic mechanisms underlying the coupling of the dendritic with the axonal action potential initiation zone of adult rat layer 5 pyramidal neurons. *J Physiol (Lond)* 533:447–466
- Linden DJ (1999) The return of the spike: postsynaptic action potentials and the induction of LTP and LTD. *Neuron* 22:661–666
- Livingstone MS (1998) Mechanisms of direction selectivity in macaque V1. *Neuron* 20(3):509–526
- Livingstone MS, Conway BR (2003) Substructure of direction-selective receptive fields in macaque V1. *J Neurophysiol* 89(5):2743–2759
- Magee JC, Johnston D (1997) A synaptically controlled, associative signal for Hebbian plasticity in hippocampal neurons. *Science* 275:209–213
- Markram H, Lübke J, Frotscher M, Sakmann B (1997) Regulation of synaptic efficacy by coincidence of postsynaptic APs and EPSPs. *Science* 275:213–215
- Mel B (1994) Information processing in dendritic trees. *Neural Comput* 6:1031–1085
- Mo CH, Gu M, Koch C (2004) A learning rule for local synaptic interactions between excitation and shunting inhibition. *Neural Comput* 16(12):2507–2532
- Movshon JA (1975) The velocity tuning of single units in cat striate cortex. *J Physiol* 249(3):445–468
- Movshon JA, Thompson ID, Tolhurst DJ (1978) Spatial summation in the receptive fields of simple cells in the cat's striate cortex. *J Physiol* 283:53–77
- Nishiyama M, Hong K, Mikoshiba K, Poo M, Kato K (2000) Calcium release from internal stores regulates polarity and input specificity of synaptic modification. *Nature* 408:584–588
- Orban G (1984) *Neuronal operations in the visual cortex*. Springer, Heidelberg
- Orban GA, Kennedy H, Maes H (1981) Velocity sensitivity of areas 17 and 18 of the cat. *Acta Psychol (Amst)* 48(1–3):303–309
- Pack CC, Conway BR, Born RT, Livingstone MS (2006) Spatiotemporal structure of nonlinear subunits in macaque visual cortex. *J Neurosci* 26(3):893–907
- Pettigrew JD, Nikara T, Bishop PO (1968) Responses to moving slits by single units in cat striate cortex. *Exp Brain Res* 6(4):373–390
- Poirazi P, Brannon T, Mel B (2003) Arithmetic of subthreshold synaptic summation in a model cal pyramidal cell. *Neuron* 37:977–987
- Porr B, Wörgötter F (2003) Isotropic sequence order learning. *Neural Comput* 15:831–864
- Priebe NJ, Ferster D (2005) Direction selectivity of excitation and inhibition in simple cells of the cat primary visual cortex. *Neuron* 45(1):133–145
- Reid RC, Soodak RE, Shapley RM (1991) Directional selectivity and spatiotemporal structure of receptive fields of simple cells in cat striate cortex. *J Neurophysiol* 66(2):505–529
- Royer S, Pare D (2003) Conservation of total synaptic weight through balanced synaptic depression and potentiation. *Nature* 422:518–522
- Saudargiene A, Porr B, Wörgötter F (2004) How the shape of pre- and postsynaptic signals can influence STDP: a biophysical model. *Neural Comput* 16:595–626
- Saudargiene A, Porr B, Wörgötter F (2005) Local learning rules: predicted influence of dendritic location on synaptic modification in spike-timing-dependent plasticity. *Biol Cybern* 92:128–138
- Senn W, Buchs NJ (2003) Spike-based synaptic plasticity and the emergence of direction selective simple cells: mathematical analysis. *J Comput Neurosci* 14:119–138
- Sherman I, Spitzer H (1995) Model of local velocity in the primary visual cortical cells. *J Opt Soc Am A Opt Image Sci Vis* 12(6):1198–1207
- Shon AP, Rao RP, Sejnowski TJ (2004) Motion detection and prediction through spike-timing dependent plasticity. *Network* 13(3):179–198
- Sillito AM (1977) Inhibitory processes underlying the directional specificity of simple, complex and hypercomplex cells in the cat's visual cortex. *J Physiol* 271(3):699–720
- Sjöström PJ, Turrigiano GG, Nelson SB (2001) Rate, timing, and cooperativity jointly determine cortical synaptic plasticity. *Neuron* 32:1149–1164
- Stuart G, Spruston N (1998) Determinants of voltage attenuation in neocortical pyramidal neuron dendrites. *J Neurosci* 18(10):3501–3510
- Tolhurst DJ, Dean AF (1991) Evaluation of a linear model of directional selectivity in simple cells of the cat's striate cortex. *Vis Neurosci* 6(5):421–428
- Tomita S, Stein V, Stocker TJ, Nicoll RA, Brecht DS (2005) Bidirectional synaptic plasticity regulated by phosphorylation of stargazin-like TARPs. *Neuron* 45(2):269–277
- Wenisch OG, Noll J, Hemmen JL (2005) Spontaneously emerging direction selectivity maps in visual cortex through STDP. *Biol Cybern* 93(4):239–247
- Wimbauer S, Wenisch OG, van Hemmen JL, Miller KD (1997a) Development of spatiotemporal receptive fields of simple cells: II. Simulation and analysis. *Biol Cybern* 77(6):463–477
- Wimbauer S, Wenisch OG, Miller KD, van Hemmen JL (1997b) Development of spatiotemporal receptive fields of simple cells: I. Model formulation. *Biol Cybern* 77(6):453–461